Genetic Diversity and Connectivity of Reef-Building *Halimeda macroloba* in the Indo-Pacific Region

Xiaohan Song , Jianting Yao , Michael Y. Roleda , Yanshuo Liang , Yude Lin , Yuqun Du , Delin Duan *

Posted Date: 24 March 2025

doi: 10.20944/preprints202503.1688.v1

Keywords: population genetic structure; gene flow; ocean currents; calcified algae; seaweed conservation

Article

Genetic Diversity and Connectivity of Reef-Building *Halimeda macroloba* in the Indo-Pacific Region

Xiaohan Song [1,2], Jianting Yao [1], Michael Y. Roleda [3], Yanshuo Liang [4], Yude Lin [1], Yuqun Du [5] and Delin Duan [1,2,*]

[1] Key Laboratory of Breeding Biotechnology and Sustainable Aquaculture, Institute of Oceanology, Chinese Academy of Sciences, Qingdao 266000, China

[2] Laboratory for Marine Biology and Biotechnology, Qingdao Marine Science and Technology Center, Qingdao 266200, China

[3] Algal Ecophysiology (AlgaE) Laboratory, Marine Science Institute, University of the Philippines, Quezon City 1101, the Philippines

[4] Laboratory of Marine Organism Taxonomy and Phylogeny, Qingdao Key Laboratory of Marine Biodiversity and Conservation, Institute of Oceanology, Chinese Academy of Sciences, Qingdao 266071, China

[5] Melbourne Integrative Genomics, School of Biosciences, University of Melbourne, Melbourne, VIC 3010, Australia

* Correspondence: dlduan@qdio.ac.cn

Abstract: Understanding the population genetic connectivity is crucial for the sustainability and persistence of marine biodiversity. As fundamental reef-building macroalga in the coastal ecosystem, *Halimeda macroloba* is one of dominant intertidal seaweed in the Indo-Pacific region. However, the genetic structure and population connectivity haven't been recognized yet. Here, we explored the population genetic structure and genetic connectivity of *H. macroloba* using chloroplast *tuf*A, *rps*3-*rpl*14 and *rbc*L. Our results indicated low genetic diversity and shallow population genetic structure at the intraspecific level, uncovering 3 genetic groups with 5 subdivided lineages in *tuf*A and 2 genetic clusters in *rps*3-*rpl*14. We detected demographic expansion in the last glacial period of Pleistocene and significantly asymmetric gene flow among different geographical units. We suggested that the southwestward ocean currents under the influence of northeast monsoon in the Indo-Pacific region was the main reason for shaping the present genetic structure; and the asexual reproduction of *H. macroloba* also played an important role of the low genetic diversity pattern; as well, the divergence between genetic clusters might be related to the historical isolation led by the paleoclimate oscillation in Pleistocene. The Xisha islands in southern China might serve as a potential refugium of *H. macroloba*, which needs extra attention to the conservation management. Given the limitation of sample size, we'll conduct more field work and carry out further research at larger scale in the future. Our study shed light into the theory of population connectivity in the Indo-Pacific region, and provided scientific basis for the tropical costal seaweed conservation.

Keywords: population genetic structure; gene flow; ocean currents; calcified algae; seaweed conservation

1. Introduction

The introduction should briefly place the study in a broad context and highlight why it is.

Connectivity conservation is essential for maintaining biodiversity and adapting to climate change across all biomes and spatial scales [1,2]. Increasing connectivity can increase ecosystem resilience and facilitate population recovery [3]. Compared with terrestrial ecosystems, the marine ecosystems have higher dynamic and spatial heterogeneity, and it is difficult to distinguish habitat

 doi:10.20944/preprints202503.1688.v1

patches between different ecosystems, which undoubtedly increases the difficulty of biological connectivity research and application [4]. In recent years, the intensive anthropogenic activities and climate changes led to the loss and fragmentation of coastal ecosystems [5], which has forced us to accelerate the researches on coastal connectivity to develop better conservation strategies.

As crucial producer of the coastal ecosystem, the seaweeds possess substantial economic, ecological, and social value, which provide essential resources such as food, medicine, oxygen, shelter, and habitat for both humans and marine organisms [6]. As highly calcareous green algae, *Halimeda* serves as one of the most important reef-building macroalgae in the global coastal coral reef ecosystem [7–9]. Recent studies have pointed that the *Halimeda* species underwent intricate evolutionary history related to the paleoclimate oscillation in the Indo-Pacific region [10,11], which is a well-known hotspot of marine biodiversity around the world with complex geological history, coastal topography, hydrological conditions and marine environment [12]. However, the research on intraspecific genetic connectivity of *Halimeda* species in the tropical coastal waters is still lacking. Consequently, studying the genetic connectivity of *Halimeda* species can provide insight into the conservation of calcified algae resources in the Indo-Pacific region, and provide scientific evidence for the protection of tropical coral reef ecosystems.

Among them, the *Halimeda macroloba* Decaisne acts as an important carbonate contributer in the tropical intertidal ecosystem [13]. *Halimeda macroloba* is widely distributed in the Indo-Pacific region, and functions as the dominant species in the Thai-Malay peninsula, with the distribution pattern affected by the water depth, sea surface temperature and phosphate concentration [14]. Previous studies have demonstrated that it seemed to harbor low genetic variation in the Indo-Pacific region [15,16], but the genetic connectivity at intraspecific level remain poor acknowledged.

In this study, we investigated the genetic diversity and population structure of *H. macroloba* in the Indo-Pacific region using the chloroplast *tuf*A, *rps*3-*rpl*14, and *rbc*L genes, and estimated mechanism of the genetic connectivity maintaining present distribution patterns at the intraspecific level. Our results could enrich the tropical seaweed genetic theory, and aid the understanding for the biodiversity conservation of reef-building macroalgae.

2. Results

2.1. Genetic Diversity and Population Genetic Structure

We obtained 191 *tuf*A sequences and 175 *rps*3-*rpl*14 sequences, with 12 and 6 haplotypes, respectively (Table 1). Unexpectedly, the amplification of *rbc*L was challenging and we eventually obtained 25 sequences and 2 haplotypes (Table 1). Apart from two Chinese populations (YX and TP) that displayed moderate haplotype diversity in *tuf*A, all other populations exhibited the pattern of low haplotype diversity and low nucleotide diversity. (Table 1).

 doi:10.20944/preprints202503.1688.v1

Table 1. Molecular diversity inferred from chloroplast *tuf*A, *rps*3-*rpl*14 and *rbc*L of *Halimeda macroloba* in the Indo-Pacific region.

Country	ID	Sample sites	Coordinates	Source	*tuf*A				*rps*3-*rpl*14				*rbc*L			
					n	N_h	*H*d	π (×10^{-2})	*n*	N_h	*H*d	π (×10^{-2})	*n*	N_h	*H*d	π (×10^{-2})
China	YX	Yongxing Island, Xisha Islands, Sansha, Hainan	16.83°N, 112.33°E	This study	9	4	0.694±0.147	0.104±0.090	9	2	0.500±0.129	0.170±0.120	-	-	-	-
China	TP	Taiping Island, Gaoxiong, Taiwan	10.38°N, 114.37°E	GenBank	3	2	0.667±0.314	0.078±0.097	-	-	-	-	-	-	-	-
Viet Nam	CD	Con Dao, Ba Ria-Vung Tau	8.69°N, 106.62°E	GenBank	1	1	0	0	-	-	-	-	-	-	-	-
Viet Nam	NTH	Ninh Thuan	15.66°N, 109.18°E	GenBank	1	1	0	0	-	-	-	-	-	-	-	-
Viet Nam	PQ	Phy Quy	10.55°N, 108.96°E	GenBank	1	1	0	0	-	-	-	-	-	-	-	-
Viet Nam	NTR	Nha Trang	12.22°N, 109.2°E	GenBank	1	1	0	0	-		-	-	-	-	-	-
Thailand	CB	SamaeSan village, Chon Buri	12.60°N, 100.95°E	This study	21	1	0	0	9	1	0	0	-	-	-	-
Thailand	KSN	Big Buddha, Koh Samui (North coast)	9.57°N, 100.06°E	This study	25	1	0	0	24	1	0	0	1	1	0	0
Thailand	KSE	Koh Tean (East), Koh Samui, Suratthani	9.38°N, 99.95°E	This study	20	4	0.363±0.131	0.046±0.050	17	2	0.118±0.101	0.010±0.019	1	1	0	0
Thailand	PK	Tangkhen Bay, Phuket	7.81°N, 98.41°E	This study	30	1	0	0	30	1	0	0	11	1	0	0
Thailand	ST	Koh LiDi, Satun	6.79°N, 99.77°E	This study	24	1	0	0	18	3	0.216±0.124	0.019±0.026	4	1	0	0
Malaysia	ML	Pulau Besar, Malacca	2.11°N, 102.34°E	This study	30	2	0.067±0.061	0.008±0.018	29	1	0	0	8	2	0.250±0.180	0.084±0.072
the Philippines	MPH	Sablayan, Mindoro	12.86°N, 120.75°E	This study	25	4	0.230±0.110	0.037±0.043	20	2	0.269±0.113	0.023±0.029	-	-	-	-

n, sample size; N_h, number of haplotypes; *H*d, haplotype diversity; π, nucleotide diversity; -, null.

 doi:10.20944/preprints202503.1688.v1

Due to the limited number of *rbc*L sequences available for population analysis, we utilized the *tuf*A and *rps*3-*rpl*14 datasets to investigate the population genetic structure. In *tuf*A, the congruent results of the haplotype network and PCoA analysis indicated the presence of three genetic groups in the Indo-Pacific region (Figure 1). Group A contained the populations including China, Vietnam, and the Philippines (Figure 1). Group B included the populations along the coast of Thailand and Malaysia, with the exception of Phuket (PK) in Thailand, which was the only population in Group C corresponding to lineage 5 (Figure 1). Moreover, while a monophyletic origin was identified, the intraspecific phylogenetic relationship exhibited limited divergence, with five sub-lineages detected (Figure 1C). The YX population consisted of haplotypes from four lineages, acting as the place with richest genetic diversity in the studying area, which was located in Xisha islands of China (Figure 1A; Table 1).

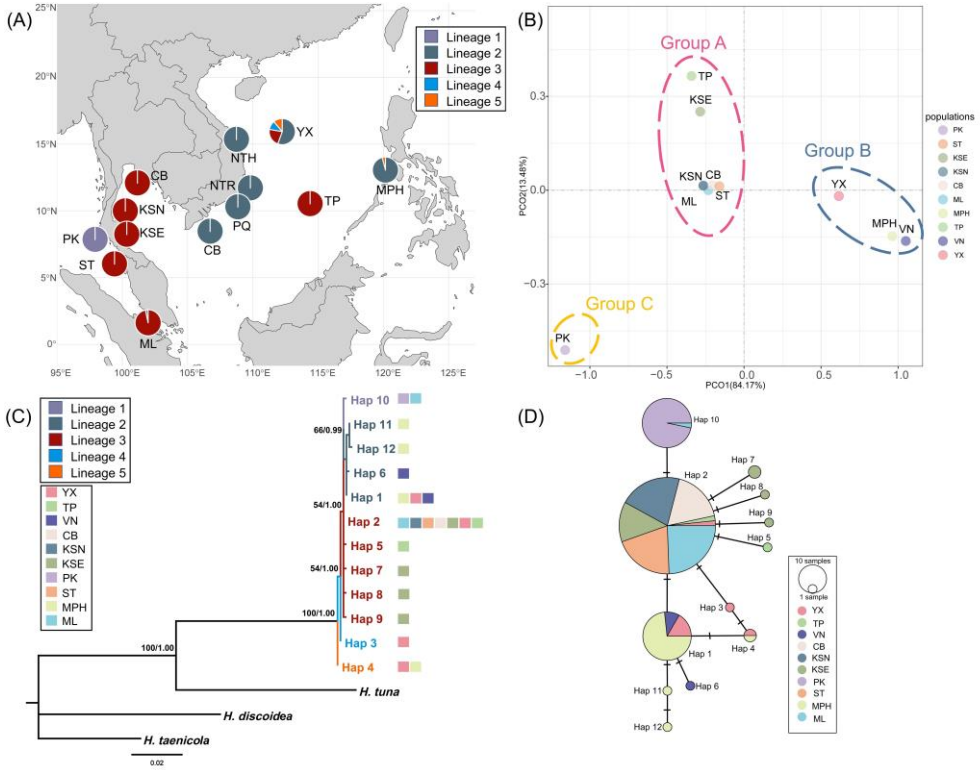

Figure 1. The phylogeographical structure of *H. macroloba* in *tuf*A. (A) The geographical distribution of 5 lineages in the Indo-Pacific region. (B) Population genetic structure based on PCoA analysis. (C) Phylogenetic relationship of *H. macroloba* based on *tuf*A haplotypes. Numbers above or near branches are ML bootstrap values (left) / BI posterior probabilities (right). Values <50% or <0.50 were not shown. (D) Median-joining network based on *tuf*A haplotypes. The circle size represented the sample sizes. The number of bars on the connecting lines represented the genetic steps.

In *rps*3-*rpl*14, concordant patterns were observed across the population genetic structure, phylogenetic relationship, and the haplotype network, which indicated two genetic clusters at the intraspecific level (Figure S1). The group A occurred in Chinese and Philippine populations (YX and MPH), and the group B covered the entire Thai-Malay peninsula and central South China Sea (Figure S2).

In order to examine the genetic differentiation of *H. macroloba*, we complemented the AMOVA and pairwise *F*st analyses both on *tuf*A and *rps*3-*rpl*14. The AMOVA results showed that the genetic differentiation mainly occurred among genetic groups and within populations (Table S2). The pairwise *F*st of *tuf*A suggested that most populations had obvious genetic differentiation, and in particular, the differentiations between populations belonging to different genetic groups were more significant (Figure 2A). The pairwise *F*st of *rps*3-*rpl*14 showed consistency with the genetic structure

 doi:10.20944/preprints202503.1688.v1

that significant genetic differentiation was observed between populations from different groups, whereas no considerable differentiation was detected among populations within the same group (Figure 2B).

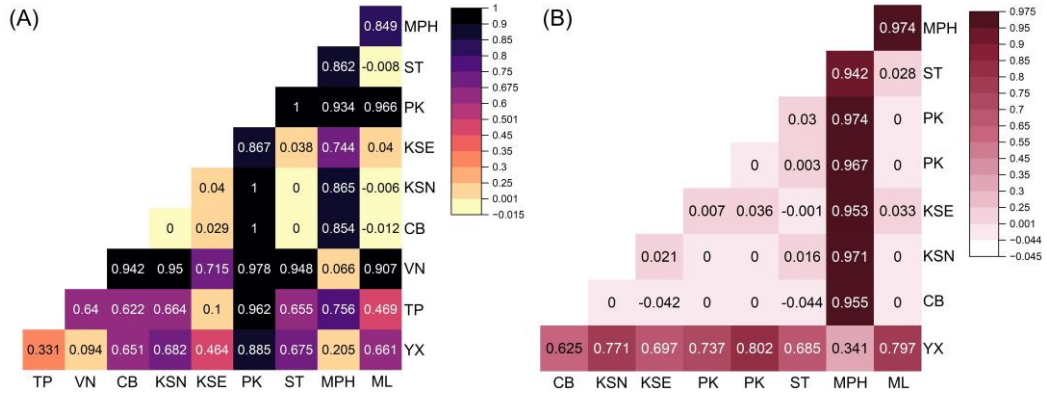

Figure 2. Pairwise genetic differentiation (*F*st) between populations based on *tuf*A (A) and *rps*3-*rpl*14 (B).

2.2. Demographical Population History

With the timeframe proposed by Verbruggen et al. (2009) [63], the *Halimeda* genus was diverged at about 144 Myr before present. Therefore, we calibrated that the molecular clock of *tuf*A and *rps*3-*rpl*14 as 0.078%/Myr and 0.043%/Myr respectively. Mismatch analysis showed unimodal distribution patterns based on *tuf*A and *rps*3-*rpl*14, which supported the recent demographical expansion model (Figure 3A & B). Furthermore, in Bayesian skyline plots (BSP) analyses, the intraspecific dynamics initiated approximately 0.223 Myr ago both in *tuf*A and *rps*3-*rpl*14 (Figure 3C & D). Corresponding to the results of mismatch analysis, demographic expansions were detected in both markers. In *tuf*A, we found persistent expansion from 0.223 Myr ago (Figure 3C); in *rps*3-*rpl*14, we found that *H. macroloba* remained stable during a long period and then expanded rapidly from about 0.05 Myr ago (Figure 3D).

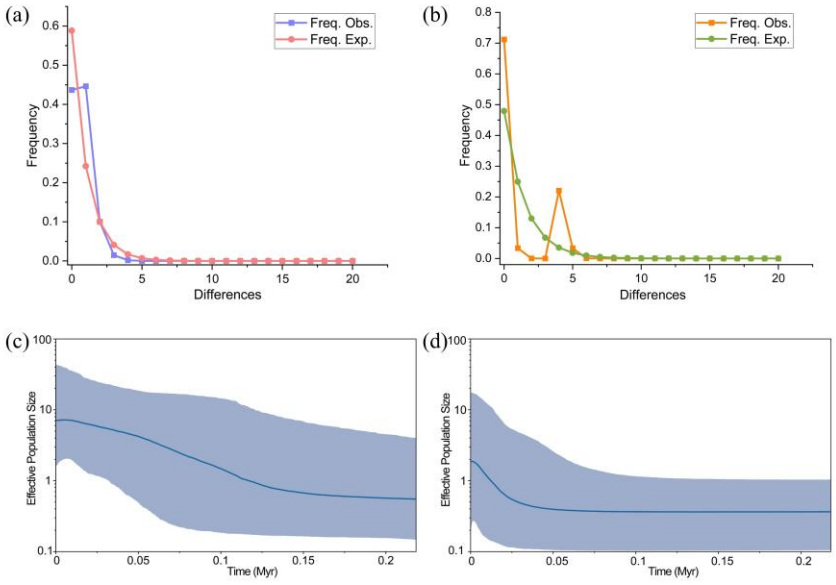

Figure 3. Demographic dynamics of *H. macroloba* in *tuf*A and *rps*3-*rpl*14. (A) Mismatch distribution of *tuf*A. (B) Mismatch distribution of *rps*3-*rpl*14. (C) BSP results of *tuf*A. The horizontal axis represented the past time in the unit of per million years (Myr), and the vertical axis represented the effective population size. The blue intervals represented the 95% highest posterior density (HPD). The blue curve represented the median value. (D) BSP results of *rps*3-*rpl*14. The horizontal axis represented the past time in the unit of per million years (Myr), and the

 doi:10.20944/preprints202503.1688.v1

vertical axis represented the effective population size. The blue intervals represented the 95% highest posterior density (HPD). The blue curve represented the median value.

2.2. Population Gene Flow

We used the *tuf*A dataset to infer the population gene flow (*Nm*) due to more extensive geographical populations than *rps*3-*rpl*14 dataset. The Bayesian migration analysis inferred from *tuf*A revealed asymmetric gene flow among the sub-units in the Indo-Pacific region (Figure 4). On the one hand, we found high level of genetic exchange in the vast South China Sea region, including two Chinese populations (1, 2), Vietnamese populations (3) and Philippine population (4). Strong bidirectional gene flow was detected among these four units, with migration rates exceeding 20 in all units and even above 30; besides, it indicated that the westward and southward gene flow between all the units was greater than the opposite direction. On the other hand, asymmetric gene flow occurred between the populations in the South China Sea region and the populations in the Gulf of Thailand and the Malacca Strait. Gene flow from Vietnam (3) to the Gulf of Thailand (5) was significantly higher than that in the opposite direction (3→5: *Nm* = 24.03; 5→3: *Nm* = 1.22) (Figure 4). Meanwhile, gene flow from Vietnam (3) to the Malacca Strait (7) was also significantly higher than that in the opposite direction (3→7: *Nm* = 26.22; 7→3: *Nm* = 0.43) (Figure 4). In addition, we found limited genetic exchange between the units of the Gulf of Thailand and the Malacca Strait; notably, the genetic exchange between these units was still mainly from east to west (5→6: *Nm* = 1.44; 6→5: *Nm* = 0.06; 5→7: *Nm* = 1.64; 7→5: *Nm* = 0.55) (Figure 4).

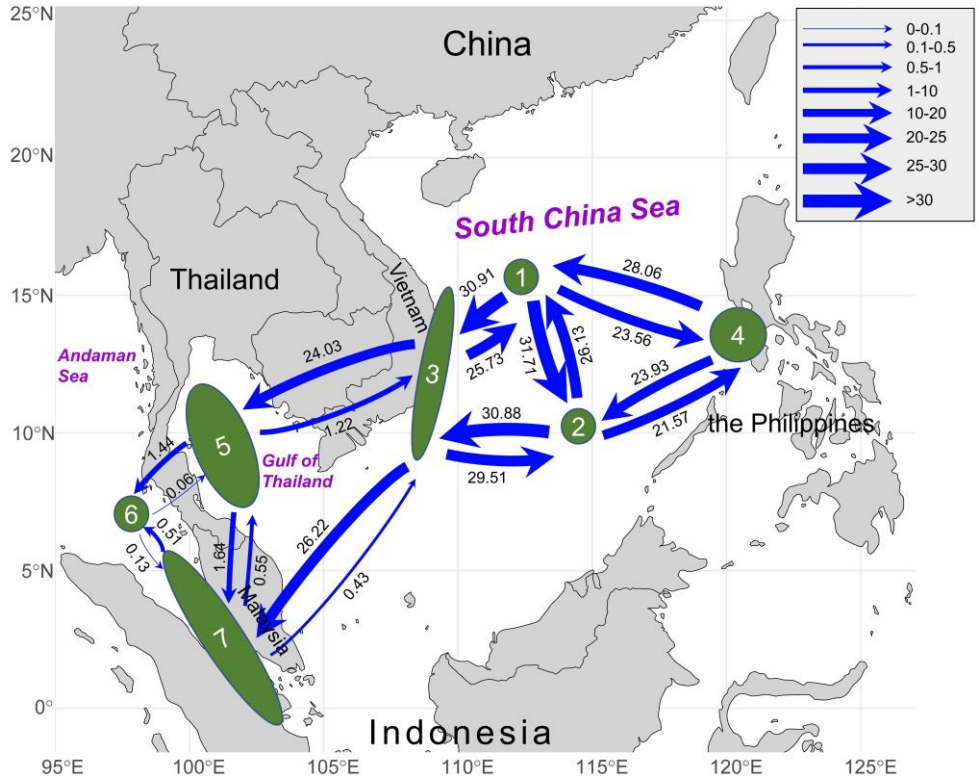

Figure 4. Gene flow (*Nm*) between 7 sub-units based on *tuf*A. Numbers above/below the arrows represented migration rates in the direction of the arrow. Arrow thickness was scaled according to the value.

3. Discussion

3.1. Genetic Connectivity Derived by Ocean Currents

Genetic diversity serves as a fundamental pillar for ecosystem resilience, facilitating species adaptation to environmental changes, and underpinning nature's essential contributions to human [17,18]. Among marine organisms, the population connectivity has a significant impact on the

 doi:10.20944/preprints202503.1688.v1

differentiation and population genetic structure [19]. The ocean currents can facilitate gene flow between populations to promote genetic homogeneity; conversely, they can also lead to increased genetic differentiation among populations as physical barriers [20–22]. Based on the 3 chloroplast molecular datasets, the molecular diversity within *H. macroloba* displayed a pattern of low genetic diversity (Table 1). Meanwhile, we discovered shallow population genetic structure and strong gene flow at intraspecific level (Figures 1, 4 and S1). The species exhibiting high fecundity and dispersal capabilities usually lack significant spatial genetic structure [23]. Therefore, the phylogeographical pattern of *H. macroloba* was likely caused by the influence of ocean currents in the Indo-Pacific region.

Our integrated results suggested that the gene flow directionality was corresponding to the ocean currents of the northeast monsoon in the Indo-Pacific region. In the northern and central parts of South China Sea, the bidirectional gene flow was strong between populations (1, 2, 3 and 4) (Figure 4). We speculated that the genetic exchange was frequent due to the lack of a dispersal barrier in the vast South China Sea. Meanwhile, the gene flow from the populations of South China Sea to populations of Gulf of Thailand and Andaman Sea exhibited a significant southwestward pattern (Figure 4). Such genetic connectivity pattern might be mediated by the southwest surface circulations in this region. Affected by the seasonal monsoon climate in the Indo-Pacific region, the ocean current system was complicated and intense, characterized by opposite flow directions in winter and summer; the surface circulation in winter flows mainly from northeast to southwest, which could facilitate the genetic exchange at the intraspecific level [24]. Particularly, in winter, the coastal Vietnam are among the regions with the strongest currents at the scale of the South China Sea basin, where the southwestward drift velocities could exceed 1 m/s [25,26]. It might explain the formation of the strong gene flow observed from unit 3 to 5 and 7. On the western coast of Thai-Malay peninsula, the limited gene flow between units 6 and 7 might be related to the hydrological conditions along the Malacca Strait during winter monsoon. Located within the equatorial doldrums, the current of the Malacca Strait is influenced by the equatorial low-pressure zone and the topography of coastline, resulting in generally weak surface flows. It likely accounted for the limited genetic exchange between units in this region. Under the impact of the winter monsoon, the surface current in the Malacca Strait generally moves from the southeast to the northwest towards the Andaman Sea (flowing from areas of higher to lower water volume), which corresponds to the stronger northward gene flow from units 7 to 6 [27]. Similar conditions were documented in other seaweed species and adjacent seas. For *Sargassum* species with high capability of dispersal (air vesicles providing positive buoyancy), the ocean currents also played a dominant role in their genetic structure [28,29]; furthermore, the southwestern current in the Indo-Pacific region might act as a critical factor affecting their dispersal and colonization [30,31]. Our results demonstrated the importance of ocean currents in shaping the genetic connectivity of marine plants. Nevertheless, many researches illustrated that the seaweed in the Indo-Pacific region hold rich genetic diversity and highly divergent structure, implying limited genetic exchange between different populations [32,33]; some researches indicated that genetic differentiation might arise from the topographical isolation and hydrological barrier of Thai-Malay peninsula [34–36]. Therefore, extensive sample collection and further integrated study are needed to shed light into the theory of seaweed genetic connectivity here.

On the other hand, we discovered that while the genetic homogeneity was high along the Thai-Malay peninsula, the gene flow was limited here, and in the *tuf*A dataset, there was only 1 haplotype in Phuket population (PK) in Thailand, which was divergent from other populations as an independent genetic cluster (Figures 1B and 4). We assumed that the notably low genetic diversity may be associated with the asexual reproduction of *H. macroloba*. Previous study revealed that *Halimeda* species primarily reproduce asexually in natural environment, and the abundant biomass on coral reefs is partially due to the ability of this genus to propagate asexually via vegetative fragmentation [37]. Thus, we suggested that the separate genetic cluster in Phuket might be the consequence of a local enrichment of one unique haplotype by vegetative fragmentation.

 doi:10.20944/preprints202503.1688.v1

3.2. Intraspecific Phylogeographical Pattern of H. macroloba

Based on the 3 chloroplast molecular datasets, the molecular diversity within *H. macroloba* displayed a pattern of low haplotype diversity and low nucleotide diversity (Table 1). However, we discovered more genetic variations in *tuf*A dataset than *rps*3-*rpl*14. Therefore, the *tuf*A gene marker might have a higher resolution in population genetic research and retained more historical relics in the evolutionary process. Three genetic groups and five subdivided genetic lineages were found in *tuf*A, and four lineages were located in the Xisha islands (YX) in southern China (Figure 1A). Additionally, the YX population displayed highest haplotype diversity in this study (Table 1). The populations in glacial refugia usually retained higher genetic diversity and particular haplotypes than recolonized populations [38]. Hence, we hypothesized that for *H. macroloba*, the Xisha Islands might serve as a potential historical refugium, which highlighted the value of extra conservation and management here. But, due to the limited sample size of this population, the reliability of the hypothesis couldn't be guaranteed. In previous researches of other marine organisms, the Xisha islands was regarded as a transfer station for genetic exchange rather than a diversity center [39]. It's necessary to enlarge the collection range and quantity to ensure the accuracy of research results.

Besides, the low genetic diversity and simple phylogeographical pattern could be correlated with historical expansion. Recent rapid expansion might lead to the simplification of genetic structure. The star-like haplotype network and unimodel distribution in mismatch together supported the population expansion, and the BSP directly showed obvious expansion occurred during the Pleistocene. Despite the lack of high divergence, we still found genetic structures in different datasets (Figures 1 and S1). So the present genetic structure may also be related to the historical isolation caused by sea level fluctuation in Pleistocene. Based on the BSP results, the divergence of this species in the Indo-Pacific region originated from 0.223 Myr ago (Figure 3C,D), which roughly coincided with the emergence of Sundaland (0.15-0.25 Myr ago) [40,41]. The Sundaland acted as a geographical barrier for marine organisms on both sides, which might result in the genetic differentiation of the populations between South China Sea basin and Thai-Malay peninsula. Continuous expansion was detected in *tuf*A dataset while intraspecific expansion sharply increased from 0.05 Myr ago in the *rps*3-*rpl*14 (Figure 4C,D). It suggested that the species underwent a complex historical process during the last glacial period during the Pleistocene, and the current genetic structure may be the consequence of historical isolation and genetic mixture through sea level fluctuation [42–44].

3.3. Conservation and Management

The low genetic diversity and simple population genetic structure underscored the importance of genetic diversity protection of *H. macroloba*. We proposed to divide two management units (MU) of South China Sea basin and Thai-Malay peninsula for separate conservation [45]. Moreover, due to the higher haplotype diversity of Xisha population in China and distinct genetic cluster of Phuket population in Thailand, we suggested more attention should be paid based on current marine conservation strategies.

4. Materials and Methods

4.1. Sample Collection, DNA Extraction and Amplification

From 2019 to 2024, we collected *H. macroloba* samples in the Indo-Pacific convergence region along the coast of China, Thailand and the Philippines (Figure 1A). Total genomic DNA was extracted using the Hi-DNAsecure Plant Kit (TIANGEN, DP350-03) following the manufacturer's instruction, and the quality was checked using 0.7% agarose gel electrophoresis and OD260/OD280 ratio.

The chloroplast-encoded *tuf*A, *rps*3-*rpl*14, and *rbc*L were amplified as molecular markers. For *tuf*A, the amplification was carried out using the primer pairs *tuf*A-F (5′-TGAAACAGAAMAWCGTCATTATGC-3′) and *tuf*A-R (5′-CCTTCNCGAATMGCRAAWCGC-3′)

 doi:10.20944/preprints202503.1688.v1

[46] and the PCR procedures in Cremen et al. (2016) [47]. For *rps*3-*rpl*14, the amplification was carried out with the primers *rps*3F (5′-ACACAACCGCATTTATCACA-3′) and *rpl*14R (5′-CAGCAACATTWACAYAACTTTCAG-3′) and the PCR procedures in Rindi et al. (2020) [48]. For *rbc*L, the amplification was carried out with the primers U1-1 and U3-2 [49], and the PCR procedures was performed according to the procedures by Curtis et al. (2008) [50]. The PCR products were checked in 1% agarose gel electrophoresis. Purification and sequencing of PCR products were performed using a BigDye Terminator Cycle sequencing kit and an ABI3730 automated sequencer (Applied Bio-systems, Foster City, CA, USA).

4.2. Molecular Diversity and Phylogenetic Relationship

The obtained sequence datasets were aligned with MUSCLE model in MEGA X respectively [51]. After manual adjusting for false or missing gaps, we computed the haplotype diversity, nucleotide diversity, variable sites and parsimony informative sites for all populations in Arlequin 3.5.2.2 [52].

After testing the optimal substitution model of each dataset based on Corrected Akaike Information Criterion (AICc) in JModelTest 2.1.7 [53], we reconstructed the phylogenetic relationships of each dataset based on with Maximum Likelihood (ML) and Bayesian Inference (BI). Phylogenetic ML trees were constructed based on 1000 bootstrap replicates using a Nearest-Neighbor-Interchange heuristic method in PhyML 3.1 [54]. The BI trees were constructed based on 10,000,000 MCMC iteration chains with the first 2,500,000 chains discarded as 'burn-in' in Beast 2.7.5 [55]. The convergence of output trees dataset was checked in Tracer 1.7.1 [56] when the effective sample sizes (ESS) >200. The condensed tree was summarized in TreeAnnotator in Beast 2.7.5 with a 25% "burn-in". The sequences of congeneric species *H. discoidea* Decaisne and *H. taenicola* W.R.Taylor were selected as outgroups (accession number in GenBank: AY826362 and AY826365). All trees were visualized using FigTree 1.4.4 (http://tree.bio.ed.ac.uk/software/Figtree/).

4.3. Population Genetic Structure and Differentiation

We estimated the population pairwise differentiation (*F*st) with 1000 permutations in Arlequin. The genealogic network diagrams based on the haplotypes of each dataset were drawn using Median-Joining algorithm in POPART [57].

The population genetic structure of each dataset was detected based on the admixture model in STRUCTURE 2.3.4 [58]. The optimal number of clusters was tested using putative K value from 1 to 8. The analysis carried out 10 repetitive iterations per K with a burn-in of 100,000 MCMC chains followed by 500,000 chains using a correlated allele frequencies model [59]. The log-likelihood LnP(K) and statistic ΔK [60] was estimated to determine the most probable K value by online Structure Harvester (http://taylor0.biology.ucla.edu/struct_harvest/).

To further check the hierarchical structure and distinctiveness, a principal component analysis (PCoA) was operated in GenAlex 6.5.2.2 based on the population pairwise genetic distances both in *tuf*A and *rps*3-*rpl*14 [61]. And the analysis of molecular variance (AMOVA) was conducted to explore the genetic differentiation of subdivisions based on the result of population genetic structure.

4.4. Divergence Time and Demographic History

We conducted the mismatch analysis using *tuf*A and *rps*3-*rpl*14 datasets in DnaSP v5.0 [62] to assess the historical population dynamics. We calibrated the molecular clock of *H. macroloba* using the timeframe proposed by Verbruggen et al. (2009) [63]. The divergence time of *Halimeda* genus was estimated as 144 Myr ago, so we calculated the substitution rates of *tuf*A and *rps*3-*rpl*14 based on the genetic divergence between haplotypes of *Halimeda* species (*H. macroloba* and *H. discoidea*).

Aiming to study the population demographic history, the coalescent Bayesian skyline plots (BSPs) analysis was proceeded in Beast v2.6.6 based on *tuf*A and *rps*3-*rpl*14. Molecular clocks of the two genes were chosen as relaxed clock log normal with calculated substitution rates. MCMC chains

 doi:10.20944/preprints202503.1688.v1

were set as 8×10^8 iterations, followed by 2×10^8 iterations discarded as burn-in, with sampling every 80,000 iterations.

4.5. Intraspecific Genetic Connectivity

In order to investigate the gene flow between populations, we estimated the migration rates and effective population size based on *tuf*A datasets in Migrate-n 4.4.3 [64]. We delineated 7 sub-units corresponding to the geographical distributions and population genetic structure (shown in Figure 4 of Results section). The analysis was conducted based on four long chains and ten replicates with a 10,000 'burn-in' and a total of 50,000 steps along with sampling per 100 steps. Heating was set with four temperatures (1.0, 1.5, 3.0, and 1.0) with a static scheme.

Supplementary Materials: The following supporting information can be downloaded at: www.mdpi.com/xxx/s1. Figure S1: The phylogeographical structure of *H. macroloba* in *rps*3-*rpl*14. (A) The geographical distribution of 5 lineages in the Indo-Pacific region. (B) Phylogenetic relationship of *H. macroloba* based on *rps*3-*rpl*14 haplotypes. Numbers above or near branches are ML bootstrap values (left) / BI posterior probabilities (right). Values <50% or <0.50 were not shown. (C) Median-joining network based on *tuf*A haplotypes. The circle size represented the sample sizes. The number of bars on the connecting lines represented the genetic steps. (D) Population genetic structure based on PCoA analysis. Table S1: Analysis of molecular variance (AMOVA) based on *tuf*A and *rps*3-*rpl*14.

Author Contributions: DDL, YJT and SXH conceived the research. YJT, RMY and LYD collected specimens. SXH, LYS and DYQ conducted molecular experiments. SXH adjusted and analyzed the data. SXH performed the phylogeographical analysis. SXH and DDL wrote and revised the manuscript. All authors have read and agreed to the published version of the manuscript.

Funding: This research was supported by the Strategic Priority Research Program of Chinese Academy of Sciences (XDB42030203), the Thailand Research Fund (RDG6130002) and the Qingdao Postdoc Project (QDBSH20240102101).

Data Availability Statement: The newly discovered *tuf*A haplotypes of *H. macroloba* in this study could be found in GenBank with the accession numbers: PQ824573-PQ824582. The *rps*3-*rpl*14 haplotypes has been submitted to GenBank with a submission ID 2939450. The *rbc*L haplotypes has been submitted to GenBank with a submission ID 2939478. The newly discovered *tuf*A sequences of *H. discoidea* in this study has been submitted to GenBank with a submission number 2917045.

Acknowledgments: We thanked the members of the Seagrass & Seaweed Research Unit of the Prince of Songkla University (Hat Yai, Thailand) for their help with sampling. We thanked Dr. Eka S. Prasedya in University of Mataram (Indonesia) for the help with *H. discoidea* collection. And we thanked Dr. Stefano G. A. Draisma in the Prince of Songkla University for the revision and polish of English writing of this manuscript.

Conflicts of Interest: The authors declare no conflicts of interest.

Abbreviations

The following abbreviations are used in this manuscript:

AICc	Akaike Information Criterion
ML	Maximum Likelihood
BI	Bayesian Inference
ESS	effective sample sizes
PCoA	Principal component analysis
AMOVA	analysis of molecular variance
BSP	Bayesian skyline plots
Nm	Migration rates
Myr	million years
MU	management unit

 doi:10.20944/preprints202503.1688.v1

References

1. Jones, G. P.; Srinivasan, M.; Almany, G. R. Population connectivity and conservation of marine biodiversity. *Oceanography* 2007, *20* (3), 100-111. DOI: 10.5670/oceanog.2007.33
2. IUCN-WCPA. Guidelines for conserving connectivity through ecological networks and corridors. 2020, https://iucn.org/resources/publication/guidelines-conserving-connectivity-through-ecological-networks-and-corridors
3. Krosby, M.; Tewksbury, J.; Haddad, N. M.; et al. Ecological connectivity for a changing climate. *Conserv Biol* 2010, *24* (6), 1686-1689. DOI: 10.1111/j.1523-1739.2010.01585.x
4. Steele, J. H.; Brink, K. H.; Scott, B. E. Comparison of marine and terrestrial ecosystems: suggestions of an evolutionary perspective influenced by environmental variation. *ICES J Mar Sci* 2019, *76* (1), 355-355. DOI: 10.1093/icesjms/fsy186
5. Hughes, T. P.; Baird, A. H.; Bellwood, D. R.; et al. Climate change, human impacts, and the resilience of coral reefs. *Science* 2003, *301* (5635), 929-933. DOI: 10.1126/science.1085046
6. Kemppainen, P.; van Nes, S.; Ceder, C.; et al. Refuge function of marine algae complicates selection in an intertidal snail. *Oecologia* 2005, *143* (3), 402-411. DOI: 10.1007/s00442-004-1819-5
7. Wefer, G. Carbonate production by algae *Halimeda*, *Penicillus* and *Padina*. *Nature* 1980, *285* (5763), 323-324. DOI: 10.1038/285323a0
8. Rees, S. A.; Opdyke, B. N.; Wilson, P. A.; et al. Significance of *Halimeda* bioherms to the global carbonate budget based on a geological sediment budget for the Northern Great Barrier Reef, Australia. *Coral Reefs* 2007, 26 (1), 177-188. DOI: 10.1007/s00338-006-0166-x
9. Nelson, W. A. Calcified macroalgae - critical to coastal ecosystems and vulnerable to change: a review. *Mar Freshwater Res* 2009, 60 (8), 787-801. DOI: 10.1071/MF08335
10. Verbruggen, H.; Tyberghein, L.; Pauly, K.; et al. Macroecology meets macroevolution: evolutionary niche dynamics in the seaweed. *Global Ecol Biogeogr* 2009, 18 (4), 393-405. DOI: 10.1111/j.1466-8238.2009.00463.x
11. Zhang, H.; Wang, X.; Qu, M.; et al. Genome of *Halimeda opuntia* reveals differentiation of subgenomes and molecular bases of multinucleation and calcification in algae. *P Natl Acad Sci USA* 2024, 121 (39). DOI: 10.1073/pnas.2403222121
12. Du, Y.; Wang, F.; Wang, T. Y.; et al. Multi-scale ocean dynamical processes in the Indo-Pacific Convergence Zone and their climatic and ecological effects. *Earth-Sci Rev* 2023, 237. DOI: 10.1111/pre.12361
13. Mayakun, J.; Prathep, A. Calcium carbonate productivity by *Halimeda macroloba* in the tropical intertidal ecosystem: The significant contributor to global carbonate budgets. *Phycol Res* 2019, 67 (2), 94-101. DOI: 10.1111/pre.12361
14. Stankovic, M.; Draisma, S. G. A.; Pongparadon, S.; et al. Predicting macroalgal species distributions along the Thai-Malay Peninsula. *Estuar Coast Shelf S* 2022, 267. DOI: 10776010.1016/j.ecss.2022.107760
15. Pongparadon, S.; Zuccarello, G. C.; Phang, S. M.; et al. Diversity of *Halimeda* (Chlorophyta) from the Thai-Malay Peninsula. *Phycologia* 2015, 54 (4), 349-366. DOI: 10.2216/14-108.1
16. Nguyen, T. H.; Nguyen N. N. T.; Nguyen X. T.; et al. Morphological variation and haplotype diversity of *Halimeda macroloba* and *H. opuntia* (Chlorophyta: Halimedaceae) from southern Vietnam. *Viet Acad Sci Tech* 2022, 22 (2), 165–176.
17. Des Roches, S.; Pendleton, L. H.; Shapiro, B.; et al. Conserving intraspecific variation for nature's contributions to people. *Nat Ecol Evol* 2021, 5 (5), 574-582. DOI: 10.1038/s41559-021-01403-517
18. Legrand, T.; Fragkopoulou, E.; Vapillon, L.; et al. Unravelling the role of oceanographic connectivity in the distribution of genetic diversity of marine forests at the global scale. *Global Ecol Biogeogr* 2024, 33 (8). DOI: 10.1111/geb.13857
19. White, C.; Selkoe, K. A.; Watson, J.; et al. Ocean currents help explain population genetic structure. *P Roy Soc B-Biol Sci* 2010, 277 (1688), 1685-1694. DOI: 10.1098/rspb.2009.2214
20. Cardona, L.; Hays, G. C. Ocean currents, individual movements and genetic structuring of populations. *Mar Biol* 2018, 165 (1). DOI: 10.1007/s00227-017-3262-2
21. Fontana, S.; Wang, W. L.; Tseng, K. Y.; et al. Seaweed diversification driven by Taiwan's emergence and the Kuroshio Current: insights from the cryptic diversity and phylogeography of *Dichotomaria* (Galaxauraceae, Rhodophyta). *Front Ecol Evol* 2024, 12. DOI: 10.3389/fevo.2024.1346199

22. Peluso, L.; Faúndez, J.; Navarrete, S. A.; et al. Oceanographical-driven dispersal and environmental variation explain genetic structure in an upwelling coastal ecosystem. *Sci Rep* 2024, 14 (1). DOI: 2194210.1038/s41598-024-72841-x
23. Gagnaire, P. A.; Broquet, T.; Aurelle, D.; et al. Using neutral, selected, and hitchhiker loci to assess connectivity of marine populations in the genomic era. *Evol Appl* 2015, 8 (8), 769-786. DOI: 10.1111/eva.12288
24. Hu, J.; Kawamura, H.; Hong, H; et al. A Review on the Currents in the South China Sea: Seasonal Circulation, South China Sea Warm Current and Kuroshio Intrusion. *J Oceanogr* 2000, 56, 607–624. DOI: 10.1023/A:1011117531252
25. Yang, H. J.; Liu, Q. Y.; Liu, Z. Y.; et al. A general circulation model study of the dynamics of the upper ocean circulation of the South China Sea. *J Geophys Res-Oceans* 2002, 107 (C7). DOI: 10.1029/2001JC001084
26. Vlasova, G. A.; Demenok, M. N.; Xuan, N. B.; et al. The role of atmospheric circulation in spatial and temporal variations in the structure of currents in the western South China Sea. *Izv Atmos Ocean Phy* 2016, 52 (3), 317-327. DOI: 10.1134/S0001433816030130
27. Ibrahim, Z. Z.; Yanagi, T. The influence of the Andaman Sea and the South China Sea on water mass in the Malacca Strait. *La Mer* 2006, 43, 33-42.
28. Chan, S. W.; Cheang, C. C.; Chirapart, A.; et al. Homogeneous population of the brown alga *Sargassum polycystum* in Southeast Asia: possible role of recent expansion and asexual propagation. *Plos One* 2013, 8 (10). DOI: 10.1371/journal.pone.0077662
29. Li, J. J.; Hu, Z. M.; Gao, X.; et al. Oceanic currents drove population genetic connectivity of the brown alga *Sargassum thunbergii* in the north-west Pacific. *J Biogeogr* 2017, 44 (1), 230-242. DOI: 10.1111/jbi.12856
30. Liang, Y. S.; Zhang, S. S.; Yan, C. X.; et al. Influence of Indo-Pacific ocean currents on the distribution and demographic patterns of the brown seaweed *Sargassum polycystum* in tropical east Asia. *Front Mar Sci* 2022, 9. DOI: 10.3389/fmars.2022.895554
31. Lin, Y. D.; Zhang, J.; Du, Y. Q.; et al. Marine conditions in Andaman Sea shape the unique genetic structure of *Sargassum plagiophyllum* C. Agardh. *J Appl Phycol* 2024, 36 (1), 501-511. DOI: 10.1007/s10811-023-03144-3
32. Boo, G. H.; Leliaert, F.; Le Gall, L.; et al. Ancient Tethyan vicariance and long-distance dispersal drive global diversification and cryptic speciation in the red seaweed *Pterocladiella*. *Front Plant Sci* 2022, 13. DOI: 10.3389/fpls.2022.849476
33. Lagourgue, L.; Leliaert, F.; Payri, C. E. Historical biogeographical analysis of the Udoteaceae (Bryopsidales, Chlorophyta) elucidates origins of high species diversity in the Central Indo-Pacific, Western Indian Ocean and Greater Caribbean regions. *Mol Phylogenet Evol* 2022, 169. DOI: 10.1016/j.ympev.2022.107412
34. Wichachucherd, B.; Prathep, A.; Zuccarello, G. C. Phylogeography of *Padina boryana* (Dictyotales, Phaeophyceae) around the Thai-Malay Peninsula. *Eur J Phycol* 2014, 49 (3), 313-323. DOI: 10.1080/09670262.2014.918658
35. Pongparadon, S.; Zuccarello, G. C.; Phang, S. M.; et al. Diversity of *Halimeda* (Chlorophyta) from the Thai-Malay Peninsula. *Phycologia* 2015, 54 (4), 349-366. DOI: 10.2216/14-108.1
36. Bulan, J.; Maneekat, S.; Zuccarello, G. C.; et al. Phylogeographic patterns in cryptic species (Rhodomelaceae, Rhodophyta) across the Thai-Malay Peninsula. *Algae* 2022, 37 (2), 123-133. DOI: 10.4490/algae.2022.37.6.4
37. Walters, L. J.; Smith, C. M.; Coyer, J. A.; et al. Asexual propagation in the coral reef macroalga *Halimeda* (Chlorophyta, Bryopsidales): production, dispersal and attachment of small fragments. *J Exp Mar Biol Ecol* 2002, 278 (1), 47-65. DOI: 10.1016/S0022-0981(02)00335-0
38. Maggs, C. A.; Castilho, R.; Foltz, D.; et al. Evaluating signatures of glacial refugia for north Atlantic benthic marine taxa. *Ecology* 2008, 89 (11), S108-S122. DOI: 10.1890/08-0257.1
39. Huang, W. H.; Zhang, Z. X.; Zhong, J. The genetic structure and connectivity of eight fish species in the Indo-Pacific convergence region. *J Trop Oceanogr* 2025, 44 (1), 9–23. (in Chinese with English abstract)
40. Molengraaff, G. Modern deep-sea research in the East Indian Archipelago. Geogr J 1921, 57 (2), 95–11. DOI: 10.2307/1781559
41. Bird, M. I.; Taylor, D.; Hunt, C. Palaeoenvironments of insular Southeast Asia during the Last Glacial Period: a savanna corridor in Sundaland? *Quaternary Sci Rev* 2005, 24 (20), 2228-2242. DOI: 10.1016/j.quascirev.2005.04.004

42. Hewitt, G. The genetic legacy of the Quaternary ice ages. *Nature* 2000, 405 (6789), 907-913. DOI: 10.1038/35016000
43. Hoarau, G.; Coyer, J. A.; Veldsink, J. H.; et al. Glacial refugia and recolonization pathways in the brown seaweed. *Mol Ecol* 2007, 16 (17), 3606-3616. DOI: 10.1111/j.1365-294X.2007.03408.x
44. Hu, Z. M.; Kantachumpoo, A.; Liu, R. Y.; et al. A late Pleistocene marine glacial refugium in the south-west of Hainan Island, China: Phylogeographical insights from the brown alga. *J Biogeogr* 2018, 45 (2), 355-366. DOI: 10.1111/jbi.13130
45. Carpenter, K. E.; Barber, P. H.; Crandall, E. D.; et al. Comparative phylogeography of the coral triangle and implications for marine management. *J Mar Biol* 2011, 396982. DOI: 10.1155/2011/396982
46. Famà, P.; Wysor, B.; Kooistra, W. H. C. F.; et al. Molecular phylogeny of the genus *Caulerpa* (Caulerpales, Chlorophyta) inferred from chloroplast *tuf*A gene. *J Phycol* 2002, 38 (5), 1040-1050. DOI: 10.1046/j.1529-8817.2002.t01-1-01237.x
47. Cremen, M. C. M.; Huisman, J. M.; Marcelino, V. R.; et al. Taxonomic revision of *Halimeda* (Bryopsidales, Chlorophyta) in south-western Australia. *Aust Syst Bot* 2016, 29 (1), 41-54. DOI: 10.1071/Sb15043
48. Rindi, F.; Pasella, M. M.; Lee, M. F. E.; et al. Phylogeography of the mediterranean green seaweed *Halimeda tuna* (Ulvophyceae, Chlorophyta). *J Phycol* 2020, 56 (4), 1109-1113. DOI: 10.1111/jpy.13006
49. Hanyuda, T.; Arai, S.; Ueda, K. Variability in the *rbc*L introns of Caulerpalean algae (Chlorophyta, Ulvophyceae). *J Plant Res* 2000, 113 (1112), 403-413. DOI: 10.1007/Pl00013948
50. Curtis, N. E.; Dawes, C. J.; Pierce, S. K. Phylogenetic analysis of the large subunit RUBISCO gene supports the exclusion of *Avrainvillea* and *Cladocephalus* from the Udoteaceae (Bryopsidales, Chlorophyta). *J Phycol* 2008, 44 (3), 761-767. DOI: 10.1111/j.1529-8817.2008.00519.x
51. Kumar, S.; Stecher, G.; Li, M.; et al. MEGA X: Molecular evolutionary genetics analysis across computing platforms. *Mol Biol Evol* 2018, 35 (6), 1547-1549. DOI: 10.1093/molbev/msy096
52. Excoffier, L.; Lischer, H. E. L. Arlequin suite ver 3.5: a new series of programs to perform population genetics analyses under Linux and Windows. *Mol Ecol Resour* 2010, 10 (3), 564-567. DOI: 10.1111/j.1755-0998.2010.02847.x
53. Darriba, D.; Taboada, G. L.; Doallo, R.; et al. jModelTest 2: more models, new heuristics and parallel computing. *Nat Methods* 2012, 9 (8), 772-772. DOI: DOI 10.1038/nmeth.2109
54. Guindon, S.; Gascuel, O. A simple, fast, and accurate algorithm to estimate large phylogenies by maximum likelihood. *Syst Biol* 2003, 52 (5), 696-704. DOI: 10.1080/10635150390235520
55. Bouckaert, R.; Vaughan, T. G.; Barido-Sottani, J.; et al. BEAST 2.5: An advanced software platform for Bayesian evolutionary analysis. *Plos Comput Biol* 2019, 15 (4). DOI: 10.1371/journal.pcbi.1006650
56. Rambaut, A.; Drummond, A. J.; Xie, D.; et al. Posterior summarization in Bayesian phylogenetics using Tracer 1.7. *Syst Biol* 2018, 67 (5), 901-904. DOI: 10.1093/sysbio/syy032
57. Leigh, J. W.; Bryant, D. POPART: full-feature software for haplotype network construction. *Methods Ecol Evol* 2015, 6 (9), 1110-1116. DOI: 10.1111/2041-210x.12410
58. Pritchard, J. K.; Stephens, M.; Donnelly, P. Inference of population structure using multilocus genotype data. *Genetics* 2000, 155 (2), 945-959. DOI: 10.1093/genetics/155.2.945
59. Falush, D.; Stephens, M.; Pritchard, J. K. Inference of population structure using multilocus genotype data: Linked loci and correlated allele frequencies. *Genetics* 2003, 164 (4), 1567-1587. DOI: 10.1093/genetics/164.4.1567
60. Evanno, G.; Regnaut, S.; Goudet, J. Detecting the number of clusters of individuals using the software STRUCTURE: a simulation study. *Mol Ecol* 2005, 14 (8), 2611-2620. DOI: 10.1111/j.1365-294X.2005.02553.x
61. Peakall, R.; Smouse, P. E. GenAlEx 6.5: genetic analysis in Excel. Population genetic software for teaching and research-an update. *Bioinformatics* 2012, 28 (19), 2537-2539. DOI: 10.1093/bioinformatics/bts460
62. Librado, P.; Rozas, J. DnaSP v5: a software for comprehensive analysis of DNA polymorphism data. *Bioinformatics* 2009, 25 (11), 1451-1452. DOI: 10.1093/bioinformatics/btp187

 doi:10.20944/preprints202503.1688.v1

63. Verbruggen, H.; Ashworth, M.; LoDuca, S. T.; et al. A multi-locus time-calibrated phylogeny of the siphonous green algae. *Mol Phylogenet Evol* 2009, 50 (3), 642-653. DOI: 10.1016/j.ympev.2008.12.018
64. Beerli, P.; Mashayekhi, S.; Sadeghi, M.; et al. Population genetic inference with MIGRATE. *Curr Protoc Bioinform* 2019, 68 (1), e87. DOI: 10.1002/cpbi.87